iJRASET
International Journal For Research in Applied Science and Engineering Technology

INTERNATIONAL JOURNAL FOR RESEARCH

IN APPLIED SCIENCE & ENGINEERING TECHNOLOGY

Volume: 3 **Issue:** XI **Month of publication:** November 2015

DOI:

www.ijraset.com

Call: 08813907089 | E-mail ID: ijraset@gmail.com

International Journal for Research in Applied Science & Engineering Technology (IJRASET)

Analysing the Effect of Unified Power Flow Controller on Power System Performance

Katta Mallikharjuna Rao[1], Chintalapudi V Suresh[2]
[1]Department of Electrical and Electronics Engineering, VVIT, Nambur, Guntur, A.P., India.

Abstract—The objective of the planning and operation of an electric power system is to satisfy the system load and energy requirement as economically as possible. Therefore, the system planner has to consider a variety of options, including Flexible AC Transmission Systems (FACTS) controllers, and they have to make decisions not only based on technical and cost considerations, but also on return of investment. FACTS controllers are characterized by their ability to have control algorithms structured to achieve multiple objectives in a transmission system. For this, an Optimal Power Flow (OPF) algorithm is considered to find a steady state operation point which minimizes generation cost, network loss etc. or maximizes social welfare or system utilization etc. while maintaining an acceptable system performance in terms of limits on generators' active and reactive powers, line flow limits, maximum output of various compensating devices etc. In this paper, the complete mathematical model for one of the advanced FACTS controller i.e. unified power flow controller (UPFC) is developed and the effect of this device on system parameters is analyzed on standard test systems with supporting numerical and graphical results.
Keywords— FACTs, Unified Power Flow Controller, Optimal location, SOSI value, Optimal power flow

I. INTRODUCTION

An electrical power system is the interconnection of several subsystems like generating sources, transmission lines, transformers, protecting equipments and consumer loads etc. The nature and structure of power system depends on political, engineering, economical and various environmental decisions. Normally, power systems are classified into two types as meshed and longitudinal systems. Meshed systems are placed in high population density area and near load centers and longitudinal systems are placed where larger power has to be transmitted over long distances towards load center. The goal of optimal power flow is to determine optimal control variables and quantities for efficient power system planning and operation. Several optimization techniques have been proposed to handle the OPF problem [1-3]. A wide variety of optimization techniques have been applied to solve the OPF problems such as nonlinear programming (NLP) [4-5], quadratic programming [6], linear programming [7], Newton-based techniques [8], sequential unconstrained minimization technique [9]. Generally NLP based procedures have many drawbacks such as insecure convergence properties and algorithmic complexity. In the recent past, the research in OPF such as interior point method (IPM) has been gaining wider attention in power system operation [10]. The interior point method is faster and more reliable for achieving feasibility and convergence and has been reported as computationally efficient, however if step size is not chosen properly, the sub-linear problem may have a solution that is infeasible in the original non-linear domain [11]. FACTS technology all over the world is playing a key role for fostering the transmission network to be utilized to its full potential. Many authors developed the methodology to incorporate FACTS devices to manage the transmission congestion [12-13].Authors proposed a novel methodology for placement of SVC and TCSC to relieve congestion in the system with improvement of static security margin [14].

A method to determine the optimal location of thyristor controlled series compensators (TCSCs) has been suggested based on real power performance index and reduction of total system VAR power losses and the device can be utilized to control congestion in the network [15]. Acharya proposed a new methodology based on LMPs differences and congestion rent for the location of series FACTS devices for congestion management [16]. A congestion management strategy for a pool electricity market model with combined operation of hydro and thermal generation companies has been proposed in [17]. An approach is proposed for transmission lines congestion management in a restructured market environment using a combination of demand response (DR) and flexible alternating current transmission system (FACTS) devices with a two-step market clearing procedure in [18]. Kumar and Sekhar proposed congestion management in the presence of FACTS devices considering loadability limits into account and comparison of UPFC with Sen transformer a new power flow controller with wide range capability of controlling power flows [19], [20]. However, the authors have considered only constant P, Q load models for study and impact of realistic load model needs to be investigated for congestion management. Optimal Power Flow (OPF) is a power full simulation tool that can be used for this

assessment studies. The OPF problem aims to achieve an optimal solution of a specific power system objective function, such as fuel cost, by adjusting the power system control variables, while satisfying a set of operational and physical constraints [21].

From the careful review of the literature it is identified that, most of the literature is concentrated in solving the optimal power flow problem using conventional methods and using swarm intelligence methods. And also, the conventional power system performance is enhanced using the conventional FACTs controllers. In this paper, unified power flow controller and its power injection model is presented with supporting numerical derivation. The power system performance in the presence of UPFC is analyzed using optimal power flow with generation fuel cost and total power losses as objective functions. The proposed OPF problem is solved using the proposed particle swarm optimization (PSO) algorithm while satisfying system equality and in-equality constraints. The developed methodology is tested on IEEE-14 bus test system with supporting numerical and graphical results.

II. MODELLING OF UPFC

The general structure of UPFC contains "back-to-back" AC to DC voltage source converters through a common DC link capacitor shown in Fig.1 [21]. First converter (CONVERTER-I) is connected in shunt and the second one (CONVERTER-II) in series with the line. The shunt converter is primarily used to provide active power demand of the series converter through a common DC link. Converter-I can also generate or absorb reactive power, if it is desired, and thereby provide independent shunt reactive compensation for the line. Converter-II provides the main function of the UPFC by injecting a voltage with controllable magnitude and phase angle in series with the line.

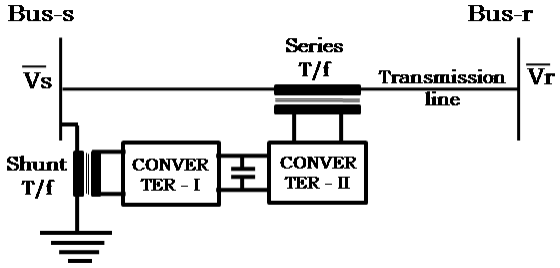

Fig.1 Principle configuration of UPFC

A. Power Injection Model Of UPFC

UPFC can be represented by two voltage sources which are controllable in both magnitude and phase angle and are representing fundamental components of output voltages of two converters and impedances being leakage reactances of two coupling transformers. Let us define two UPFC buses s and r as shown in Fig.2. For the analysis purpose, it is assumed that voltage at bus-s is taken as $\overline{V_s} = V_s \angle \delta_s$.

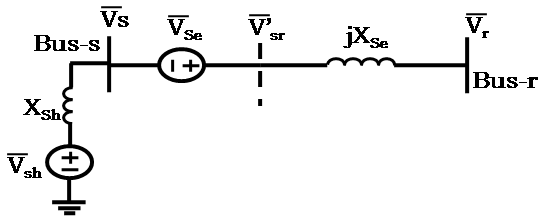

Fig.2 Equivalent voltage source model of UPFC

The controllable series voltage source $\overline{V_{se}}$ is defined as

$$\overline{V}_{se} = r\overline{V}_s e^{j\gamma} \quad (1)$$

where 'r' and 'γ' are respective per unit magnitude and phase angles of series voltage source and which operate in the following specified limits

$$0 \le r \le r_{\max} \text{ and } 0 \le \gamma \le \gamma_{\max}$$

Volume 3 Issue XI, November 2015
ISSN: 2321-9653
International Journal for Research in Applied Science & Engineering Technology (IJRASET)

The UPFC device is incorporated in between two PQ buses, out of which one is a common bus for both of the converters. Briefly, the series converters are connected between bus-s and bus-r and shunt converter is connected at bus-s. The UPFC power injection model is developed in two stages, one is series connected voltage source model and the other is shunt connected voltage source model.

The voltage behind the series reactance is calculated as

$$\overline{V'}_{sr} = \overline{V}_s + \overline{V}_{se} \tag{2}$$

B. Series Connected Voltage Source Model

According to Norton's theorem, the series connected voltage source model is developed by replacing the voltage source '$\overline{V_{se}}$' with an equivalent current source '$\overline{I_{se}}$' in parallel with a transmission line susceptance 'B_{se}' as shown in Fig.3.

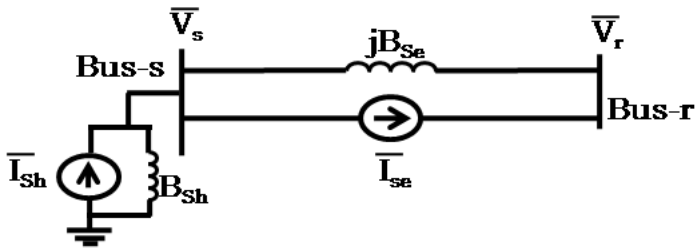

Fig.3 Equivalent current source model of UPFC

Where,

$$B_{se} = \frac{1}{jX_{se}} \tag{3}$$

'X_{se}' is the series transformer equivalent reactance

The amount of current flowing from the source is given as

$$\overline{I}_{se} = \frac{\overline{V}_{se}}{jX_{se}} = -jB_{se}\overline{V}_{se} \tag{4}$$

Replacing $\overline{V_{se}}$ in Eqn. (4) from Eqn. (1), we obtain

$$\overline{I}_{se} = -jrV_sB_{se}e^{j(\delta_s+\gamma)} = -rV_sB_{se}e^{j(90^0+\delta_s+\gamma)}$$

hence

$$(\overline{I}_{se})^* = -rV_sB_{se}e^{-j(90^0+\delta_s+\gamma)} \tag{5}$$

This current source can be modelled by injecting equivalent powers at the respective buses to which the device is connected. The corresponding power injections are shown in Fig.4.

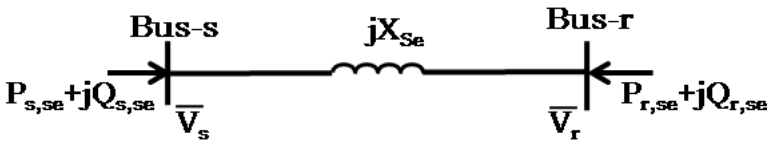

Fig.4 Equivalent series connected voltage source model

This model can be seen as the two independent complex powers injections at the UPFC buses and can be written as

$$\overline{S}_{s_{se}} = -\overline{V}_s\left(\overline{I}_{se}\right)^* \tag{6}$$

$$\overline{S}_{r_{se}} = \overline{V}_r\left(\overline{I}_{se}\right)^* \tag{7}$$

The detailed expressions for these injections can be deduced by substituting Eqn. (5) in Eqn's. (6) and (7)

$$\overline{S}_{s_{se}} = rV_s^2B_{se}e^{-j(90^0+\gamma)}$$

Volume 3 Issue XI, November 2015
ISSN: 2321-9653
International Journal for Research in Applied Science & Engineering Technology (IJRASET)

$$\overline{S}_{r_{se}} = -rV_sV_rB_{se}e^{-j(90^0+\delta_s-\delta_r+\gamma)}$$

by using Euler's identity, $e^{j\alpha} = \cos\alpha + j\sin\alpha$; let us define $\delta_{sr} = \delta_s - \delta_r$

$$\overline{S}_{s_{se}} = rV_s^2B_{se}(\cos(90^0+\gamma) - j\sin(90^0+\gamma)) \quad (8)$$

$$\overline{S}_{r_{se}} = -rV_sV_rB_{se}(\cos(90^0+\delta_{sr}+\gamma) - j\sin(90^0+\delta_{sr}+\gamma)) \quad (9)$$

by using trigonometric identities in Eqn's (8) and (9), the active and reactive power injections at buses s and r are

$$P_{s_{se}} = -rV_s^2B_{se}\sin(\gamma) \quad (10)$$

$$Q_{s_{se}} = -rV_s^2B_{se}\cos(\gamma) \quad (11)$$

$$P_{r_{se}} = rV_sV_rB_{se}\sin(\delta_{sr}+\gamma) \quad (12)$$

$$Q_{r_{se}} = rV_sV_rB_{se}\cos(\delta_{sr}+\gamma) \quad (13)$$

The equivalent series connected voltage source model with the corresponding power injections is shown in Fig.4.
Similarly, the amount of apparent power supplied by the series converter is derived as

$$\overline{S}_{ser} = P_{ser} + jQ_{ser} = \overline{V}_{se}(\overline{I}_{sr})^* = jrV_sB_{se}e^{j(\delta_s+\gamma)}(\overline{V}_{sr'} - \overline{V}_s)^* \quad (14)$$

Substituting Eqn. (2) in Eqn. (14) and simplifying

$$P_{ser} + jQ_{ser} = jrV_sB_{se}e^{j(\delta_s+\gamma)}(rV_se^{-j(\delta_s+\gamma)} + V_se^{-j\delta_s} - V_re^{-j\delta_r})$$
$$= jr^2V_s^2B_{se} + jrV_s^2B_{se}(\cos\gamma + j\sin\gamma) - jrV_sV_rB_{se}$$
$$(\cos(\delta_{sr}+\gamma) + j\sin(\delta_{sr}+\gamma))$$

Equating real and imaginary parts

$$P_{ser} = rV_sV_rB_{se}\sin(\delta_{sr}+\gamma) - rV_s^2B_{se}\sin\gamma \quad (15)$$

$$Q_{ser} = -rV_sV_rB_{se}\cos(\delta_{sr}+\gamma) + rV_s^2B_{se}\cos\gamma + r^2V_s^2B_{se} \quad (16)$$

C. Shunt Connected Voltage Source Model

The shunt connected voltage source can be modelled as an equivalent power injection from UPFC shunt branch to the series branch through converter-1. This model is also used to provide the converter switching losses. The reactive power injection at shunt converter is used to control/maintain the voltage level at sending end within limits. The equivalent shunt connected voltage source model with the corresponding power injections is shown in Fig.5. The total switching losses of the one converter is about 0.8-1% [21] of the power transferred through the converter. If these losses are considered, then the real power injection of the shunt converter is

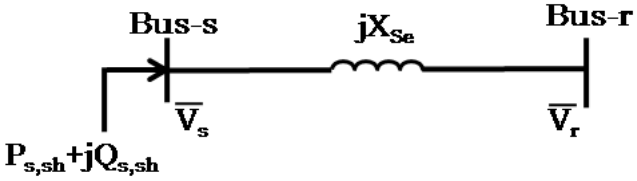

Fig.5 Equivalent shunt connected voltage source model

$$P_{s_{sh}} = -1.02P_{ser} \quad (17)$$

from Eqn's (15) and (17),

$$P_{s_{sh}} = 1.02rV_s^2B_{se}\sin\gamma - 1.02rV_sV_rB_{se}\sin(\delta_{sr}+\gamma) \quad (18)$$

Assume that constant $Q_{s_{sh}}$ is injected at bus-s. The apparent power injection at shunt branch is $\overline{S}_{s_{sh}} = P_{s_{sh}} + jQ_{s_{sh}}$.

D. Combined model

Volume 3 Issue XI, November 2015
ISSN: 2321-9653
International Journal for Research in Applied Science & Engineering Technology (IJRASET)

The final steady state power injection model of UPFC is obtained by combining series connected and shunt connected voltage source models. Then the equivalent UPFC model is shown in Fig.6. The resultant power injections are given as

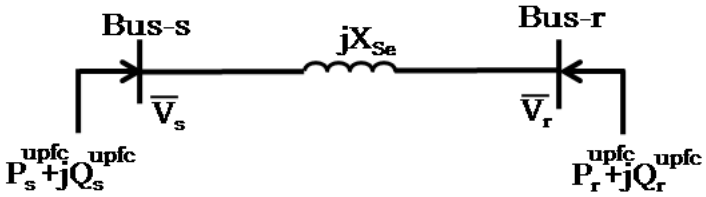

Fig.6 Equivalent power injection model of UPFC

$$P_s^{upfc} = P_{s_{se}} + P_{s_{sh}} = 0.02rV_s^2B_{se}\sin\gamma - 1.02rV_sV_rB_{se}\sin(\delta_{sr}+\gamma) \quad (19)$$

$$Q_s^{upfc} = Q_{s_{se}} + Q_{s_{sh}} = -rV_s^2B_{se}\cos\gamma + Q_{s_{sh}} \quad (20)$$

$$P_r^{upfc} = P_{r_{se}} = rV_sV_rB_{se}\sin(\delta_{sr}+\gamma) \quad (21)$$

$$Q_r^{upfc} = Q_{r_{se}} = rV_sV_rB_{se}\cos(\delta_{sr}+\gamma) \quad (22)$$

E. Power Flow In The Presence Of UPFC

To analyse the effect of UPFC on a given power system, this device is incorporated in Newton-Raphson (NR) load flow solution. The developed power injection model of UPFC is easily incorporated into the system by modifying Jacobian elements and power mismatch equations related to UPFC connected buses [21].

The final steady state network equation in NR load flow in the presence of UPFC can be expressed as

$$\left(\begin{bmatrix}\Delta P\\ \Delta Q\end{bmatrix} + \begin{bmatrix}P^{upfc}\\ Q^{upfc}\end{bmatrix}\right) = \left(\begin{bmatrix}H & N\\ J & L\end{bmatrix} + \begin{bmatrix}H^{upfc} & N^{upfc}\\ J^{upfc} & L^{upfc}\end{bmatrix}\right)\begin{bmatrix}\Delta\delta\\ \frac{\Delta V}{V}\end{bmatrix} \quad (23)$$

Where, ΔP, ΔQ are the vector corresponds to real and reactive power mismatches, Δδ, ΔV are the vector of incremental changes in angles and voltage magnitudes, H, N, J, L are the Partial derivatives of P, Q w.r.to δ, V.

The corresponding Jacobian elements and power mismatch equations related to UPFC connected buses are expressed as follows:

F. Modifications In Jacobian Elements

The diagonal and off-diagonal elements of 'H^{upfc}' are

$$H_{ss}^{upfc} = \frac{\partial P_s^{upfc}}{\partial\delta_s} = -1.02Q_r^{upfc}$$

$$H_{sr}^{upfc} = \frac{\partial P_s^{upfc}}{\partial\delta_r} = 1.02Q_r^{upfc}$$

$$H_{rs}^{upfc} = \frac{\partial P_r^{upfc}}{\partial\delta_s} = Q_r^{upfc}$$

$$H_{rr}^{upfc} = \frac{\partial P_r^{upfc}}{\partial\delta_r} = -Q_r^{upfc}$$

Similarly, the diagonal and off-diagonal elements of 'N^{upfc}' are

$$N_{ss}^{upfc} = |V_s|\frac{\partial P_s^{upfc}}{\partial V_s} = 0.02rB_{se}V_s^2\sin\gamma + P_s^{upfc}$$

$$N_{sr}^{upfc} = |V_r|\frac{\partial P_s^{upfc}}{\partial V_r} = -1.02P_r^{upfc}$$

$$N_{rs}^{upfc} = |V_s|\frac{\partial P_r^{upfc}}{\partial V_s} = Q_r^{upfc}$$

$$N_{rr}^{upfc} = |V_r|\frac{\partial P_r^{upfc}}{\partial V_r} = P_r^{sssc}$$

The diagonal and off-diagonal elements of 'J^{upfc}' are

$$J_{ss}^{upfc} = \frac{\partial Q_s^{upfc}}{\partial\delta_s} = 0$$

$$J_{sr}^{upfc} = \frac{\partial Q_s^{upfc}}{\partial\delta_r} = 0$$

$$J_{rs}^{upfc} = \frac{\partial Q_r^{upfc}}{\partial \delta_s} = -P_r^{upfc}$$
$$J_{rr}^{upfc} = \frac{\partial Q_r^{upfc}}{\partial \delta_r} = P_r^{upfc}$$

Similarly, the diagonal and off-diagonal elements of 'L^{upfc}' are

$$L_{ss}^{upfc} = |V_s|\frac{\partial Q_s^{upfc}}{\partial V_s} = 2 \times (Q_s^{upfc} - Q_{s_{sh}})$$
$$L_{sr}^{upfc} = |V_r|\frac{\partial Q_s^{upfc}}{\partial V_r} = 0$$
$$L_{rs}^{upfc} = |V_s|\frac{\partial Q_r^{upfc}}{\partial V_s} = Q_r^{upfc}$$
$$L_{rr}^{upfc} = |V_r|\frac{\partial Q_r^{upfc}}{\partial V_r} = Q_r^{upfc}$$

G. Modifications In Power Mismatch Equations

The mismatch equations in the presence of UPFC are expressed as follows (superscript `0' indicates the power mismatches without device)

$$\Delta P_s^{upfc} = \Delta P_s^0 + P_s^{upfc}$$
$$\Delta P_r^{upfc} = \Delta P_r^0 + P_r^{upfc}$$
$$\Delta Q_s^{upfc} = \Delta Q_s^0 + Q_s^{upfc}$$
$$\Delta Q_r^{upfc} = \Delta Q_r^0 + Q_r^{upfc}$$

H. Overall Computational Procedure With UPFC

The overall computational procedure of Newton-Raphson power flow method with UPFC is described in the following steps.
Read bus data, line data and UPFC data.
Assume flat voltage profile and set iteration count k=0.
Compute active and reactive power mismatch from the scheduled and calculated powers.
Determine Jacobian matrix using power flow equations.
Modify power mismatch and Jacobian elements related to UPFC connected buses to incorporate UPFC.
Solve the NR method to find the voltage magnitudes and angles correction vector.
Update the solution using correction vector.
Increase the iteration count, k=k+1.
Stop the process, if the maximum mismatch is less than given tolerance and print the output. Otherwise, go to step 3.

III. OPTIMAL LOCATION OF UPFC

Security assessment deals with determining whether or not the system operating in a normal state can withstand contingencies (such as outage of transmission lines, generators, etc.) without any limit violation. Contingency screening and ranking is one of the important components of on-line system security assessment. This thesis presents a new approach to the assessment of power system security. Using fuzzy membership functions of post contingent quantities, it quantifies the security state of a power system, which uses off-line screening for the most vulnerable system states. It introduces fuzzy composition of system severity index (FSSI) of the power system using systems variables characterized by fuzzy sets. This FSSI uses the voltage stability indices at the system buses and real power loadings of transmission lines to evaluate the system security.
The following fuzzy rules are formulated for the proposed problem formulation:

A. Transmission Line Loadings

Based on the amount of apparent power flow through the transmission lines, the transmission line loadings are divided into four categories using fuzzy set notations:
Lightly Loaded (LL) - 0-50% of the line limit (Less severe)
Normally Loaded (NL) - 50-85% of the line limit (Below severe)
Fully Loaded (FL) - 85-100% of the line limit (Above severe)

Over Loaded (OL) - >100% of the line limit (More severe)

The severity of line loadings is calculated for each of the transmission lines and after this the FLLI is obtained as:

$$FLLI = \sum_{i=1}^{N_{line}} W_{LL} SI_{LL}$$

Where, '$SI_{LL} = \frac{S_i}{S_i^{\max}}$' is the severity index of the ith line and 'W_{LL}' is the weighting coefficient for a severity index is expressed as 0.25 for LL, 0.5 for NL, 0.75 for FL and 1.00 for OL. These weights are assigned to indicate dominance of the over loaded lines and the also the importance of lightly loaded lines.

B. Bus Voltage Violations

Based on the voltage deviations available at system buses, the voltage profile fuzzy set notations are classified into three categories:

Low Voltage (LV) deviation - <0.09 p.u. (Below severe)

Normal Voltage (NV) deviation - 0.09 p.u. – 0.102 p.u. (Above severe)

Over Voltage (OV) deviation - >0.102 p.u. (More severe)

The severity of voltage profile is calculated at each of the buses and after this the overall severity index due to voltage profiles is obtained using the following equation.

$$FVDI = \sum_{i=1}^{N_{bus}} W_{VP} SI_{VP}$$

Where, $SI_{VP} = \left(\frac{V_i - V_i^{ref}}{V_i^{ref}} \right)$ is the severity index of the bus and 'W_{VP}' is the weighting coefficient for a severity index is expressed as 0.30 for LV, 0.6 for NV, 1.00 for OV. These weights are assigned to show demarcation between high voltage buses and low voltage buses.

Finally, FSSI is formulated by combining FLLI and FVDI. The diagrammatic representation of FSSI formulation is shown in Fig.7.

$$FSSI = FLLI + FVDI$$

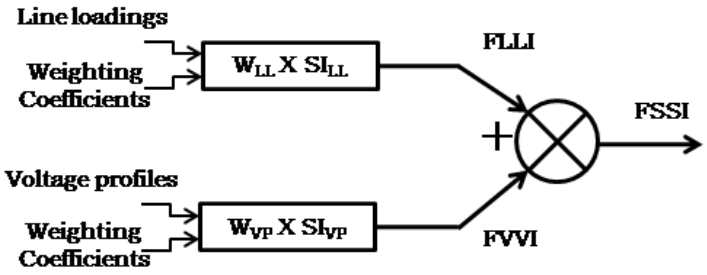

Fig.7 Representation of FSSI formulation

IV. OPF PROBLEM FORMULATION

The OPF problem aims to minimize the power system objects by adjusting the system control variables while satisfying a set of operational constraints. Therefore, the OPF problem can be formulated as follows:

$$Minimize \quad J(x,u)$$

Subjected to g(x,u)=0; h(x,u)≤0

where 'g' and 'h' are the equality and inequality constraints respectively and 'x' is a state vector of dependent variables such as slack bus active power generation ($P_{g,slack}$), load bus voltage magnitudes (V_L) and generator reactive power outputs (Q_G) and apparent power flow in lines (S_l) and 'u' is a control vector of independent variables such as generator active power output (P_G), generator voltages (V_G), transformer tap ratios (T) and reactive power output of VAr sources (Q_{sh}).

The state and control vectors can be mathematically expressed as

$$x^T = \left[P_{G_1}, V_{L_1}, \ldots\ldots V_{L_{NL}}, Q_{G_1}, \ldots\ldots Q_{G_{NG}}, S_{l_1}, \ldots\ldots S_{l_{nl}} \right]$$

$$u^T = \left[P_{G_2},.....P_{G_{NG}}, V_{G_1},.....V_{G_{NG}}, Q_{sh_1},.....Q_{sh_{NC}}, T_1,.....T_{NT}\right]$$

where, 'NL', 'NG', 'nl', 'NC' and 'NT' are the total number of load buses, generator buses, transmission lines, VAr sources and regulating transformers respectively.

A. Non-Smooth Fuel Cost Functions

The generating units with multi-valve steam turbines exhibit a greater variation in the fuel cost functions. Since the valve point results in the ripples, a cost function contains higher order nonlinearity. Therefore the cost function should be modified to consider the valve point effects. This valve point effect leads to non-smooth, non-convex input-output characteristics. Typically, the valve point results in, as each steam valve starts to open, the ripples like in to take account for the valve – point effects, sinusoidal functions are added to the quadratic cost functions as follows.

$$J_{\cos t} = \sum_{i=1}^{NG}\left(a_i P_i^2 + b_i P_i + c_i + \left|e_i \times \sin\left(f_i \times \left(P_i^{\min} - P_i\right)\right)\right|\right) \$/h \quad (24)$$

where ei and fi are the fuel cost-coefficients of the ith unit reflecting valve-point loading effects.

B. Transmission Power Loss (TPL)

The losses are calculated from the load flows. The power flow from ith bus to jth bus is given by Sij. and that for the power flow from jth bus to ith bus is given by Sji.

$$L_{ij} = S_{ij} + S_{ji} \text{ MW}$$

The total power loss bus system is given by

$$J_{TPL} = \sum_{k=1}^{nl} real(L_{ij}(k)) \text{ MW} \quad (25)$$

Where NTL is total number of transmission lines,

C. Multi-Objective Function (MOF)

A multi-objective function is formulated to get a compromised solution between generation fuel cost and total power losses, an objective function using weighted sums can be expressed as follows

$$J_{MOF} = W_1 \times J_{\cos t} + W_2 \times J_{TPL} \quad (26)$$

D. Equality Constraints

$$P_{Gk} - P_{Dm} - \sum_{m=1}^{NB}|V_k||V_m||Y_{km}|\cos\left(\theta_{km} - \delta_k + \delta_m\right) = 0 \; ; \; Q_{Gk} - Q_{Dm} + \sum_{m=1}^{NB}|V_k||V_m||Y_{km}|\sin\left(\theta_{km} - \delta_k + \delta_m\right) = 0$$

where, 'P_{Gk}, Q_{Gk}' are the active and reactive power generations at kth bus, 'P_{Dm}, Q_{Dm}' are the active and reactive power demands at mth bus, 'NB' is number of buses, |Vk|, |Vm| are the voltage magnitudes at kth and mth buses, 'δk, δm' are the phase angles of voltages at kth and mth buses, |Ykm|, θkm are the bus admittance magnitude and its angle between kth and mth buses.

E. Inequality Constraints

The following are inequality constraints for OPF problem

Generator bus voltage limits: $V_{G_i}^{\min} \le V_{G_i} \le V_{G_i}^{\max}; \quad \forall i \in N_G$

Active Power Generation limits: $P_{G_i}^{\min} \le P_{G_i} \le P_{G_i}^{\max}; \quad \forall i \in N_G$

Transformers tap setting limits: $T_i^{\min} \le T_i \le T_i^{\max}; \quad i = 1,2,..., n_t$

Capacitor reactive power generation limits: $Q_{Sh_i}^{\min} \le Q_{Sh_i} \le Q_{Sh_i}^{\max}; \quad i = 1,2,...., n_C$

Transmission line flow limit: $S_{l_i} \le S_{l_i}^{\max}; \quad i = 1,2,...., N_{line}$

Reactive Power Generation limits: $Q_{G_i}^{\min} \le Q_{G_i} \le Q_{G_i}^{\max}; \quad \forall i \in N_G$

Bus voltage magnitude limits: $V_i^{\min} \le V_i \le V_i^{\max} \quad i = 1,2,...., N_{load}$

Finally the above proposed problem is more generalized to solve in-equality constraints can be given as

$$J_{aug} = J + R_1\left(P_{g,slack} - P_{g,slack}^{\lim}\right)^2 + R_2\sum_{i=1}^{NL}\left(V_i - V_i^{\lim}\right)^2 + R_3\sum_{i=1}^{NG}\left(Q_{G_i} - Q_{G_i}^{\lim}\right)^2 + R_4\sum_{i=1}^{nl}\left(S_{l_i} - S_{l_i}^{\max}\right)^2$$

where, R_1, R_2, R_3 and R_4 are the penalty quotients having large positive value. The limit values are defined as

$$x^{\lim} = \begin{cases} x^{\max}, & x > x^{\max} \\ x^{\min}, & x < x^{\min} \end{cases}$$

Here 'x' is the value of $P_{g,slack}$, V_i, Q_{Gi}.

V. PARTICLE SWARM OPTIMIZATION

Kennedy and Eberhart first introduced PSO in year 1995 [22, 23]. PSO is motivated from the simulation of the behaviour of social systems such as fish schooling and birds flocking. The basic assumption behind the PSO algorithm is, birds find flocking and not individually, this leads to the assumption that information is exchange among the flocking.

The position of each agent is represented by XY-axis position and the velocity is expressed by Vx (the velocity of X-axis) and Vy (the velocity of Y-axis). Modification of the agent position is realized by the position and velocity information. PSO procedures based on the above concept can be described as follows. Bird flocking optimizes a certain objective function. Each agent knows its best value so far (p_{best}) and its XY position. Moreover, each agent knows the best value in the group (g_{best}) among p_{best} . Each agent tries to modify its position using the current velocity and the distance from p_{best} and g_{best} . The modification can be represented by the concept of velocity. Velocity of each agent can be modified by the following equation.

$$V_i^{k+1} = V_i^k + C_1 \times rand\ ()_1 \times (pbest_i - S_i^k) + C_2 \times rand\ ()_2 \times (gbest - S_i^k) \quad (27)$$

$$S_i^{k+1} = S_i^k + V_i^{k+1} \quad (28)$$

Where, V_i^{k+1}: Velocity of particle i at iteration $k+1$, V_i^k : Velocity of particle i at iteration k, S_i^{k+1} : Position of particle i at iteration $k+1$, S_i^k : Velocity of particle i at iteration k, , P_{best}: Position of particle i, G_{best}: Position of the swarm

VI. RESULTS AND ANALYSIS

In this section, the proposed methodology is tested on standard IEEE-14 bus test system with 5-machine and 20 transmission lines is considered [24]. The results are divided into two sections; First section gives the detailed power flow analysis in the presence of FACTS devices and in the later section, the detailed optimal power flow analysis in the presence of UPFC devices is presented.

In power flow analysis, for each of the bus systems, initially the system overall severity index (SOSI) is minimized in all of the possible locations in the presence of UPFC. From this, the location which has the least SOSI value is the best location to install UPFC (using the procedure described in section 2.3). Later, the variation of voltage magnitude at system buses and the variation of apparent power flow in transmission lines are obtained by varying the UPFC control parameters.

In optimal power flow analysis, the generation fuel cost, total transmission loss and the formulated multi objective optimization functions are optimized while satisfying equality, in-equality constraints and UPFC device limits. Here, the OPF problem control variables considered are, active power generation and voltages of PV buses, tap settings of transformers, reactive power generation of VAr sources and UPFC control parameters. Later, the variation of convergence characteristics is analyzed for the considered objectives. Finally the OPF problem is solved for the following three cases:

Case-1: Generation fuel cost minimization

Case-2: Total power losses minimization

Case-3: Multi-objective function minimization

Initially, the optimal location of UPFC is identified using SOSI analysis presented in section.3. In this analysis, the formulated SOSI objective function, which is a fuzzy composition of transmission line loadings, bus voltage profiles and system bus voltage stability indices, is optimized while satisfying equality, in-equality and device limits in all of the possible installation locations. The obtained SOSI values for this system in the presence of UPFC are tabulated in Table.1. From this table, it is observed that, the SOSI value obtained with UPFC between buses 13 and 14 is 720.9157. The detailed control parameters of SOSI minimized locations for without and with UPFC are tabulated in Table.2. From this table, it is observed that, the SOSI is decreased by 206.2653 with UPFC

Volume 3 Issue XI, November 2015
ISSN: 2321-9653

when compared to without UPFC.

TABLE.1. SOSI VALUES IN ALL POSSIBLE LOCATIONS WITH UPFC FOR IEEE-14 BUS SYSTEM

Location (From bus-To bus)	Minimized SOSI value with UPFC
10-11	878.2938
12-13	818.2837
13-14	720.9157

TABLE.2. OPF RESULTS OF SOSI MINIMIZATION FOR WITHOUT AND WITH UPFC FOR IEEE-14 BUS SYSTEM

S. No	Parameter		Without device	With UPFC
1	Real power generation (MW)	P_{G1}	13.7379	69.1231
		P_{G2}	109.4236	85.8253
		P_{G3}	48.9723	29.6982
		P_{G6}	34.184	35.0858
		P_{G8}	42.7685	31.3041
2	Generator voltages (p.u.)	V_{G1}	1.0057	1.0123
		V_{G2}	1.0347	0.9304
		V_{G3}	0.9967	1.0261
		V_{G6}	1.0247	0.9682
		V_{G8}	1.0827	0.9731
3	Transformer tap setting (p.u.)	T_{4-7}	0.9936	0.9066
		T_{4-9}	1.0009	0.9011
		T_{5-6}	0.9504	0.9034
4	Shunt compensator (MVAr)	Q_{C9}	26.52	12.3941
5	OSI-LL		920.725	715.0966
6	OSI-VP		6.344	5.7311
7	OSI-VSI		0.1126	0.08791
8	SOSI value		927.181	720.9157

A. Load Flow Analysis With UPFC

The optimal system and UPFC control parameters,when SOSI is minimized are updated in system and device data. In the UPFC control variables $Q_{sh,upfc}$ and X_{se} are kept fixed at 0.1 p.u. each, the control variable 'r' is varied from 0 p.u. to 0.1 p.u. in steps of 0.025 p.u. and the control variable 'γ' is varied from 0 deg to 360 deg in steps of 20 deg. The variation of bus voltage magnitude, line apparent power flows and total system power losses are shown in Figs. 8-10.

Volume 3 Issue XI, November 2015
ISSN: 2321-9653
International Journal for Research in Applied Science & Engineering Technology (IJRASET)

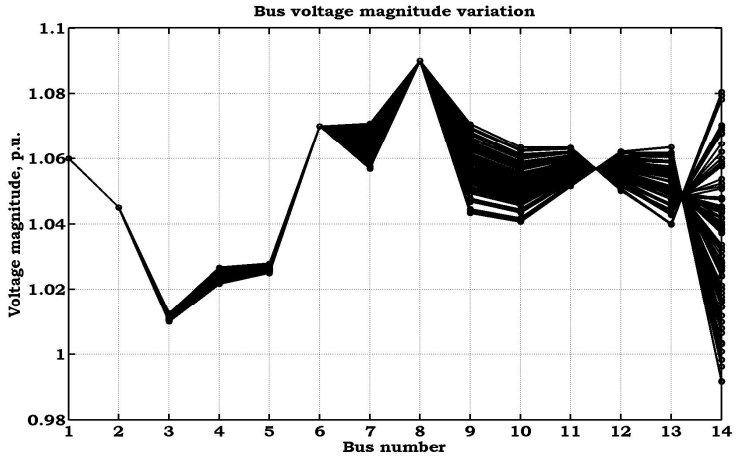

Fig.8. Variation of bus voltage magnitudes with UPFC for IEEE-14 bus system

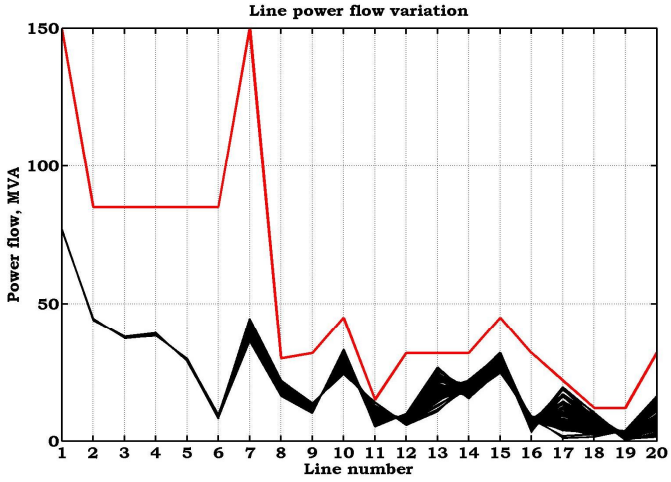

Fig.9. Variation of power flows with UPFC for IEEE-14 bus system

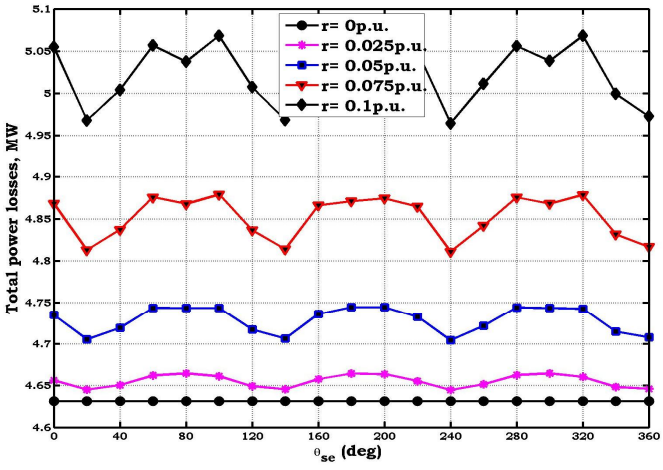

Fig.10. Variation of system losses with UPFC for IEEE-14 bus system

Volume 3 Issue XI, November 2015
ISSN: 2321-9653

From Fig.8, it is observed that, as UPFC is located between buses 13 and 14 (i.e. line-20), majority of voltage variation is observed at bus-14 when compared to remaining bus because it is device connected bus. From Fig.9, it is observed that, because of UPFC, power flow variation is high in lines 17, 18 and 20. Because these transmission lines are device connected and the nearer to the device connected location. From Fig.10, it is observed that, as `r' value is increased from 0 p.u. to 0.1 p.u.. Minimum power loss is obtained when UPFC `r' is maintained at 0 and maximum power losses obtained when `r' is at 0.1 p.u..

B. OPF Analysis With UPFC

The OPF results for the considered generation cost, TPL and multi-objective functions are tabulated in Table.3 for without and with UPFC. From this table, it is observed that, generation cost is reduced by 1.2034 $/h, TPL value is reduced by 0.0697 MW and MOF value is reduced by 0.6444 with UPFC when compared to without device. It is also observed that, while minimizing one of the objectives, the value of the other objective is increased. It is also observed that, while minimizing MOF, the generation fuel cost and TPL values are adjusted optimally so as to compromise the generation fuel cost and TPL values.

The convergence characteristics for the considered objectives without and with UPFC are shown in Figs. 11-13. From these characteristics, it is identified that, with UPFC, the convergence starts with good initial value and reaches best final value in less number of iterations when compared to without device. This is because of the effectiveness of the proposed methodology.

TABLE.3. COMPARISON OF OPF RESULTS FOR THREE CASES WITHOUT AND WITH UPFC FOR IEEE-14 BUS SYSTEM

S. No	Parameter		Case-1		Case-2		Case-3	
			Without	With	Without	With	Without	With
1	Real power Generation (MW)	P_{G1}	217.9899	219.0087	29.1835	18.1306	213.0411	214.2262
		P_{G2}	24.1011	23.9341	96.4107	105.7657	24.6614	27.0861
		P_{G3}	17.8988	16.8103	60	60	18.0079	17.5766
		P_{G6}	5.0095	5	50	50	8.7489	5.6343
		P_{G8}	5	5	25.718	27.3463	5	5
2	Generator voltages (p.u.)	V_{G1}	1.0856	1.1	1.0664	1.1	1.1	1.1
		V_{G2}	1.0529	1.0611	1.0578	0.979	0.9325	0.9398
		V_{G3}	0.9744	0.9449	1.0376	1.0489	0.9836	0.9758
		V_{G6}	1.0095	1.0309	1.0557	1.0471	1.0121	1.0029
		V_{G8}	0.9824	1.0043	1.001	0.9921	0.931	0.9401
3	Transformer tap setting (p.u.)	T_{4-7}	1.0788	1.0167	0.982	0.9791	1.0845	0.9762
		T_{4-9}	1.0361	0.9829	0.9678	0.9518	1.0802	0.9894
		T_{5-6}	0.993	0.9851	0.9779	0.9825	1.0363	0.9632
4	Shunt compensator (MVAr)	Q_{C9}	21.9261	16.9079	28.2618	20.8898	29.7211	26.5226
5	UPFC parameters	r, p.u.	-	0.0937	-	0.0999	-	0.0293
6		γ, deg	-	53.2938	-	129.2938	-	314.8893
7		X_{se}, p.u.	-	0.0239	-	0.0671	-	0.0192
8		$Q_{sh,upfc}$, p.u.	-	0.0465	-	0.0887	-	0.0656
9	Total generation, MW		269.9993	269.7531	261.3122	261.2425	269.4594	269.5232
10	Total cost, $/h		823.7581	822.5547	1131.541	1157.41	824.9172	823.5647
11	TPL, MW		10.9993	10.7531	2.3122	2.2425	10.4594	10.5232
12	MOF value		427.3787	426.6539	566.9264	579.8264	417.6883	417.0439

Volume 3 Issue XI, November 2015
ISSN: 2321-9653

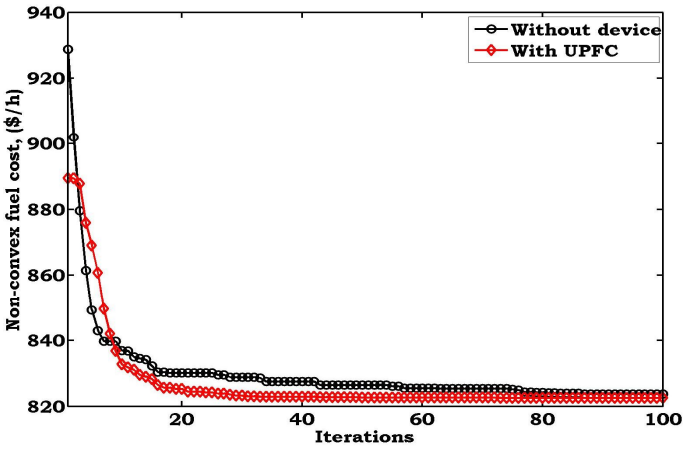

Fig.11. Convergence characteristics of generation cost with UPFC for IEEE-14 bus system

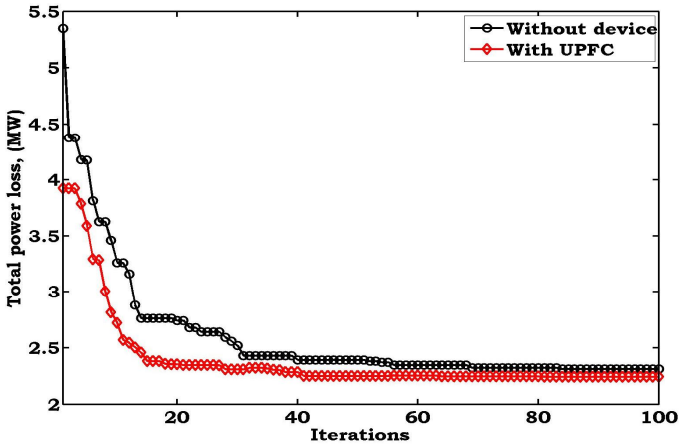

Fig.12. Convergence characteristics of TPL with UPFC for IEEE-14 bus system

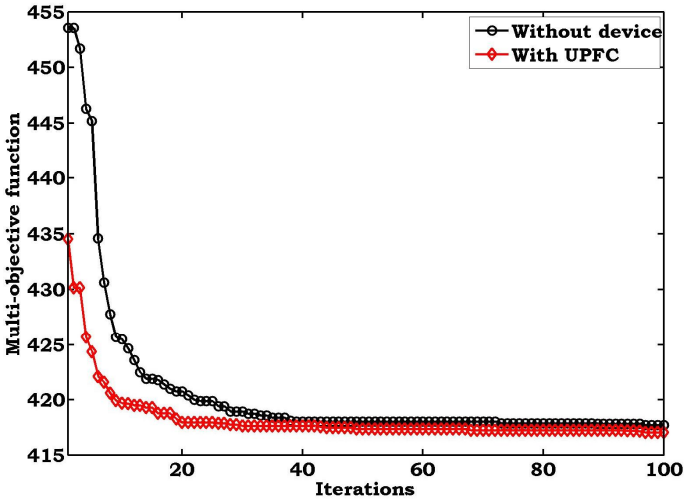

Fig.13. Convergence characteristics of multi-objective function with UPFC for IEEE-14 bus system

VII. CONCLUSIONS

In this paper, UPFC has been considered to analyze the impact of this device on system performance in terms of voltage magnitude variation at buses, power flow in the transmission lines and the total system losses. The optimal settings of this device and the system parameters have been identified by solving an optimal power flow problem. In this paper, a methodology to identify an optimal location based on the fuzzy composition of transmission line loadings, bus voltage profiles and load bus voltage stability indexes has been proposed as System Overall Severity Index (SOSI). Finally, the location in a given system which has least SOSI value with UPFC is selected as an optimal location. The variations of bus voltages, line apparent power flows and system power losses in the presence of UPFC have been observed. Similarly, the OPF problem in the presence of UPFC by considering generation fuel cost, total transmission losses as objectives in single objective OPF problems and a new multi-objective function using the above two objectives in MOP and these problems have been solved while satisfying equality and in-equality constraints using particle swarm optimization algorithm. The proposed methodology is tested in standard IEEE-14 bus test system with supporting numerical and graphical results.

REFERENCES

[1] Alsac O Stott B. “Optimal load flow with Steady State Security”. IEEE Transactionson Power Apparatus and Systems, PAS-93, 1974.
[2] C. F. Imparato A. D. Papalexopoulos and F. F. Wu. “Large scale Optimal Power Flow: Effects of initialization Decoupling and Discretization”. IEEE Transactions on Power Systems, Vol.4, 1989.
[3] J. Z. Zhu and G. Y. Xu. “A new real power economic dispatch method with security”. Electric Power Systems Research, Vol.25, 1992.
[4] Timmy W Dommel H. “Optimal power flow solution”. IEEE Transactions on Power Apparatus and Systems, PAS-87, Vol.10, 1968.
[5] Happ HH. “Optimal power dispatch: a comprehensive survey”. IEEE Transactions on Power Apparatus and Systems, PAS-96, 1977.
[6] Vierath DR Burchet RC, Happ HH. “Quadratically convergent optimal power flow”. IEEE Transactions on Power Apparatus and Systems, PAS-103, 1984.
[7] Abido MA Abou El-Ela AA. “Optimal operation strategy for reactive power control, modeling, simulation and control”. AMSE Press, Vol.41, No.3, 1992.
[8] Quintana V H. Mota-Palomino R. “Sparse reactive power scheduling by a penalty function linear programming technique”. IEEE Transactions on Power Systems, Vol.1, No.3, 1986.
[9] Da Costa GR Santos A. “Optimal power flow solution by newtons method applied to an augmented lagrangian function”. IEE Proceedings on Generation, Transmission and Distribution, Vol.142, No.1, 1995.
[10] J. C. O. Mello S. Granville and A. C. G. Melo. “Application of interior point methods to power flow unsolvability”. IEEE Transactions on Power Systems, Vol.11, 1996.
[11] Quintana VH Yan X. “Improving an interior point based OPF by dynamic adjustments of step sizes and tolerances”. IEEE Transactions on Power Systems, Vol.14, No.2, 1999.
[12] Handschin E Brosda J. “ Congestion management methods with special consideration of FACTS devices”. In: Proc. IEEE Power Tech Conf., Porto, Portugal, 2001.
[13] Sekhar Charan Kumar Ashwani. “ Congestion management with facts devices in deregulated electricity markets ensuring loadability limits”. Int J Electr Power Energy Syst, Vol.46, 2013.
[14] Yan P Huang GM. “TCSC and SVC as re-dispatch tools for congestion management and TTC improvement”. In: Proc. IEEE power engineering society winter meeting, Vol.1, 2002.
[15] Schmitt L Zhang X-Ping Yao L, Cartwright P. “Congestion management of transmission systems using FACTS”. In: Proc. IEEE/PES, Transmission and Distribution Conf. and exposition, 2005.
[16] Taher SA Besharat Haadi. “Congestion management by determining optimal location of TCSC in deregulated power systems”. Electric Power Energy Syst, Vol.30, 2008.
[17] Mithulananthan N Acharya N. “Locating series FACTS devices for congestion management in deregulated power systems”. Electric Power Energy Syst, Vol.77, 2007.
[18] Zareipour H Malik OP Yousefi A, Nguyen TT. “Congestion management using demand response and FACTS devices”. Int J Electric Power Energy Syst, Vol.37, 2012.
[19] Sekhar Charan Kumar Ashwani. “Comparison of sen transformer and UPFC for congestion management in hybrid electricity markets”. Int J Electr Power Energy Syst, Vol.46, 2013.
[20] Hajdu LP Peschon J, Bree Jr DW. “Optimal power-flow solutions for power system planning”. Proc IEEE, Vol.60, No.1, 1972.
[21] K L Lo. Mehmet Tumay, A M Vural. “The effect of unified power flow controller location in power systems”. Elecrical Power and Energy Systems, Vol.26, 2004.
[22] J. Kennedy and R. C. Eberhart. “particle swarm optimization”. Proc. of IEEE International Conference on Neural Network, 1995.
[23] M.A Abido. “optimal design of power-system stabilizers using particle swarm optimization”, IEEE Transactions on Energy Conversion, Vol.17, No.3, 2002.
[24] https://www.ee.washington.edu/research/pstca/

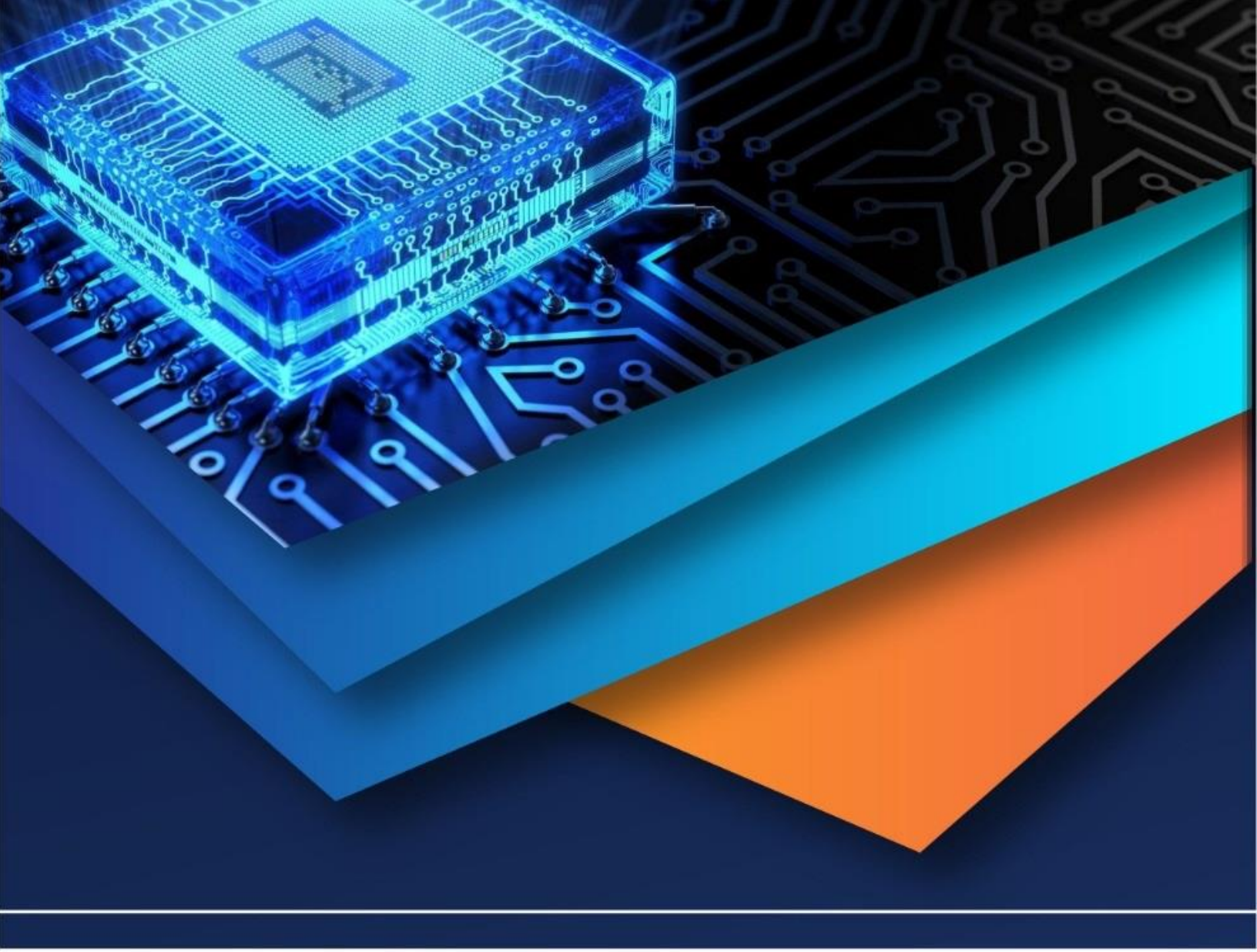

10.22214/IJRASET

45.98

IMPACT FACTOR: 7.129

IMPACT FACTOR: 7.429

INTERNATIONAL JOURNAL FOR RESEARCH

IN APPLIED SCIENCE & ENGINEERING TECHNOLOGY